ANNUAL REVIEWS

Annual Review of Condensed Matter Physics

Olfactory Sensing and Navigation in Turbulent Environments

Gautam Reddy,[1] Venkatesh N. Murthy,[2,3] and Massimo Vergassola[4,5]

[1]NSF–Simons Center for Mathematical & Statistical Analysis of Biology, Harvard University, Cambridge, Massachusetts, USA

[2]Department of Molecular & Cellular Biology, Harvard University, Cambridge, Massachusetts, USA

[3]Center for Brain Science, Harvard University, Cambridge, Massachusetts, USA

[4]Laboratoire de physique de l'École Normale Supérieure, CNRS, PSL Research University, Sorbonne Université, Paris, France; email: massimo.vergassola@phys.ens.fr

[5]Department of Physics, University of California, San Diego, La Jolla, California, USA

Annu. Rev. Condens. Matter Phys. 2022. 13:191–213

First published as a Review in Advance on November 8, 2021

The *Annual Review of Condensed Matter Physics* is online at conmatphys.annualreviews.org

https://doi.org/10.1146/annurev-conmatphys-031720-032754

Keywords

biological navigation, olfaction, fluid turbulence, odor transport, neurobiology

Abstract

Fluid turbulence is a double-edged sword for the navigation of macroscopic animals, such as birds, insects, and rodents. On the one hand, turbulence enables pheromone communication among mates and the possibility of locating food by their odors from long distances. Molecular diffusion would indeed be unable to spread odors over relevant distances in natural conditions. On the other hand, turbulent flows are hard to predict, and learning effective maneuvers to navigate them is challenging, as we discuss in this review. We first provide a summary of the olfactory organs that sense airborne or surface-bound odors, as well as the computational tasks that animals face when extracting information useful for navigation from an olfactory signal. A compendium of the dynamics of turbulent transport emphasizes those aspects that directly impact animals' behavior. The state of the art on navigational strategies is discussed, followed by a concluding section dedicated to future challenges in the field.

1. INTRODUCTION

Animals sense chemicals in their environment and use them to identify objects and locations. These chemicals or odors, sensed with specialized olfactory organs, are also used by animals to navigate toward or away from objects or locations. The strategies animals employ to navigate are likely to be different depending on the spatiotemporal distribution of chemical cues available for sampling. In this review, we discuss how odor landscapes are defined by physical properties of the world and how they constrain olfactory searches, as sketched in **Figure 1**. We restrict ourselves to terrestrial animals and emphasize navigation in naturalistic conditions, which typically involve turbulent and strongly fluctuating odor cues.

Active sampling: influencing the signal statistics, for example, by modulation of the sniffing frequency or directed movement

Olfactory sensory neurons (OSNs): sense odors through membrane receptor proteins and send axons to the first stage of brain circuit processing

Sensilla: small hairs that sense specific stimuli and project nerve fibers to the central nervous system

Endolymph: fluid that fills the sensilla to protect the dendrites of OSNs

2. HOW ARE ODORS SENSED? OLFACTORY NEUROBIOLOGY

2.1. Physical Features of Sensory Organs

Odors sensed by navigating animals are structured by environmental constraints. Chemical sensors and the organs that house them have a certain spatial extent and dynamics that define the spatiotemporal sampling of odors. Sensors vary in geometry—*Drosophila* antennae are on a scale of a millimeter and antennae of moths can measure tens of millimeters long, with a large surface area created by branching (1). In terrestrial mammals, olfactory sensory organs vary widely, and in the commonly studied olfactory animals, mice and rats, the nostrils are on a spatial scale of a centimeter. Olfactory sensing organs in higher animals come in pairs, each of which could sample independent volumes at distinct times and aid in odor navigation as we discuss below (2–6).

Animals sample odors by active inhalation of air into the nasal cavity, which houses the olfactory sensors. Odor sampling in mammals is coupled to respiration, which can be modulated voluntarily in terms of both frequency of sampling and volume sampled (7). The complex geometry of the nasal cavity and the external nostrils make it difficult to infer the details of odor transport in and around this sense organ prior to sensory transduction. Empirical and computational studies have suggested that certain physicochemical features of the odor environment might be extracted, in principle, thanks to the geometry of, and the fluid dynamics in, the nasal cavity (8–13). Evidence for such matching between the distribution of cellular sensors and the heterogeneous patterns of odors in the nasal cavity remains scarce.

Active sampling by mammals through sniffing may have parallels in insects, which can move their antennae to sample odors (1, 14, 15). Antennal movements can be induced by odors or by airflow (14), and might aid more efficient sensing, but how these movements are used for odor-guided navigation is not yet clear.

2.2. Sensory Neurons

Odorants are detected by olfactory sensory neurons (OSNs), also referred to as olfactory receptor neurons (see **Figure 2** for a schematic of the early olfactory system). In mammals, the cilia of the OSNs are embedded in the mucus layer, which is exposed to the flow in the nasal cavity (16). Molecules of odorants are transported/advected from the air to the mucus, where they are sorbed to the surface (by adsorption or absorption) and diffuse into the bulk. Insect sensory neurons are housed within structures called sensilla, which are filled with endolymph that protects the dendrites of OSNs. Olfactory binding proteins are present in high concentration in the mucus and endolymph and are thought to aid delivery of hydrophobic odorants to the aqueous environment in which the sensory neurons are embedded (17–19).

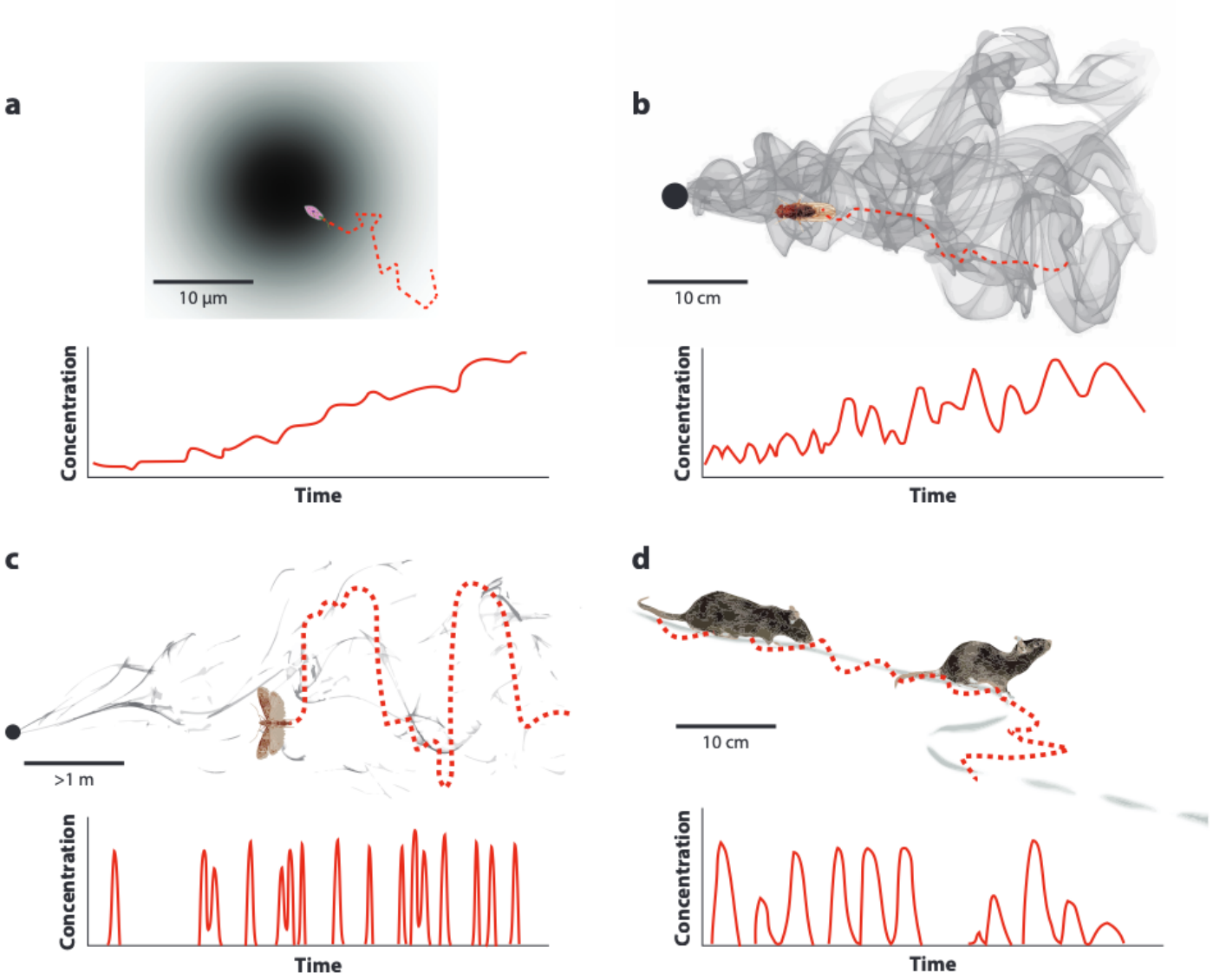

Figure 1

Odor landscapes and search strategies. The following schematic illustrates how the physics of chemical transport dictates the frequency and smoothness of stimulus encounters by navigating animals. (*a*) At microscopic scales, molecular diffusion generates smooth changes in concentrations of chemicals, allowing for gradient ascent. (*b*) In flow regimes close (tens of centimeters) to typical naturalistic sources, even if large fluctuations are present, odor concentration changes are still smooth, and an animal receives some signal most of the time. Gradient ascent strategies, or variants that approximate them, are still sufficient. (*c*) At distances on the order of meters or larger, odors are significantly dispersed such that an animal encounters stimuli infrequently and intermittently. Because local gradients are largely random in relation to the source direction at the relevant time scales, simple gradient ascent is not feasible for navigation. (*d*) Trail tracking is unique in that the stimulus is relatively stationary but spatially sparse. How animals combine ground and airborne cues by alternately sampling sniffs from the ground and in the air remains by and large unexplored.

Odorants solubilized in the mucus (or endolymph) reach the OSNs and bind to odorant receptors (ORs). This binding triggers a transduction pathway that controls the opening of plasma membrane ion channels and subsequent voltage changes in the OSN. In all species of animals investigated, ORs comprise a family with dozens to over a thousand members (20–23). The biology of ORs varies widely and includes both ligand-gated ion channels and G-protein coupled receptors (GPCRs). Several recent reviews offer summaries of many receptor families and their transduction mechanisms (24–26). A key feature of all ORs that is relevant for the topic of this

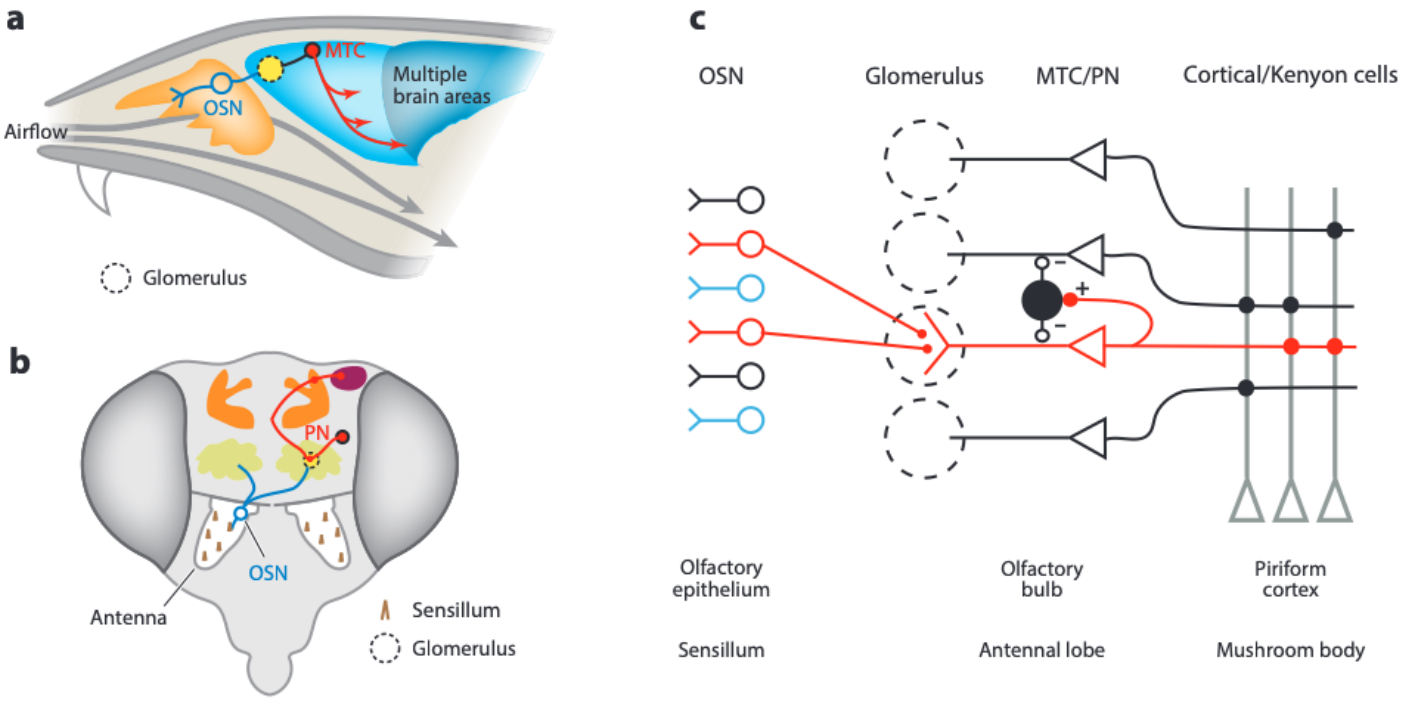

Figure 2

Scheme of neural architectures that sense and process olfactory stimuli. (*a*) Schematic of the nasal cavity and the neural components involved in olfaction in mice (sagittal plane). Airflow brings odors over the olfactory epithelium during inhalation. OSNs are electrically activated by odors and signal to the brain through their axons converging on glomeruli in the OB (*light blue*). Processed information is carried from the OB to multiple brain areas by MTCs. (*b*) Schematic of the *Drosophila* olfactory system. OSNs are housed inside structures called sensilla in the antennae (OSN shown outside sensilla for clarity) and project to the AL. PNs receive sensory input and project to multiple brain structures including the mushroom body. (*c*) Common neural circuit motif in rodents and insects. OSNs expressing a particular receptor type out of a large repertoire (indicated by like colors) converge selectively in individual glomeruli in the OB, making connections with MTCs or PNs. Local circuit elements in the OB or AL include inhibitory neurons (shown as a *black circle*) that receive excitation from MTCs/PNs and reciprocally inhibit them. MTCs/PNs project to multiple brain regions, including the piriform cortex/mushroom body, where they are thought to make dispersed, random, and sparse connections (shown as intersecting wires, with connections denoted by *small circles*). Abbreviations: AL, antennal lobe; MTCs, mitral/tufted cells; OB, olfactory bulb; OSNs, olfactory sensory neurons; PN, principal neuron.

review is their kinetics, especially under conditions of intermittent and fluctuating odor encounters likely to occur in natural conditions. The major type of ORs in mammals belongs to the GPCR family. Like other members of this family, mammalian ORs exhibit many complex properties such as agonism and antagonism for different ligands, as well as adaptation (27–33). ORs in insects are heteromeric ion channels that exhibit rapid kinetics and adaptation (34, 35). Adaptation to stimulus features has been tied to computational advantages such as preserving coding fidelity in insect ORs (36), but the functional roles of receptor adaptation in mammalian OSNs is not understood in quantitative and normative detail.

Agonists: molecules that bind to a receptor and activate the signaling pathway

Antagonists: molecules that bind to a receptor but do not activate the pathway, potentially blocking the activity of an agonist due to competitive binding

In broad terms, receptors tend to be activated by a diverse array of ligands (agonists) with different binding affinities (23) and potentially blocked by antagonists. A fundamental principle is that odorant identity is coded by a combinatorial activation of multiple receptors (22, 37), with the timing or latency of activation potentially playing a privileged role (38). Some pheromones are thought to act through dedicated receptors, but even there exclusive and selective recognition of pheromones by individual receptors is not always proven (39). Although a large fraction of studies have used single odorants to activate receptors, natural smells are mixtures of many chemical species. Several recent studies have provided strong evidence for highly nonlinear effects of

odorant mixtures, with antagonistic interactions dominating (28–33). Behavioral implications of these nonlinear interactions have yet to be fully understood (28), especially in the context of odor-guided navigation in natural environments.

The bandwidth for transmission of information about rapid fluctuations in odor concentrations by OSNs is not known for many animals. OSN responses in different insects to fluctuating stimuli suggest they can respond rapidly (40–43) and transmit several bits of information per second (44). Careful estimation of impulse response filters of OSNs in *Drosophila* points toward integration times of ∼100 ms (45).

Neural algorithms: how algorithms for odor-guided navigation are implemented in animals' brains

2.3. Neural Circuits

In most animals, individual OSNs express a single OR, and all OSNs expressing a particular OR connect to spatially local units called glomeruli (46; see **Figure 2*c***). This convergence principle is highly conserved and likely serves to reduce noise by signal averaging as well as to keep channels of information in the early stages separate. Individual glomeruli serve as relatively isolated units of sampling by second-order neurons. In structures that house glomeruli and downstream neural circuits (olfactory bulb, or OB, in mammals and antennal lobe, or AL, in insects), there is a rich network of neurons that are thought to process information with a goal of normalization, redundancy reduction, and decorrelation (47, 48). However, little attention is being paid to how this processing relates to navigational goals and the corresponding neural algorithms.

Information from the first stage (OB or AL) is passed on to multiple higher brain regions (49). An emerging theme in neuroscience is that early sensory areas have parallel output channels that send selective information about the world to different brain areas, and this is also true for the olfactory system. However, unlike the well-studied visual system (50, 51), the details of this heterogeneity are much less clear in the olfactory system. Projections from the insect AL target the mushroom body, a key center for multimodal information integration and memory formation (52), and the lateral horn, which is associated with innate behaviors (53). In mammals, the output of the OB reaches multiple areas including olfactory cortex, amygdala, and ventral striatum (49). Intriguingly, there are multiple types of OB output neurons, which have differential projection patterns, suggesting that different information is broadcast to different brain areas (54), but which of these areas are involved in odor-guided navigation is unknown.

A lot is known about the neural circuit organization in the olfactory system, with significant focus on detection and discrimination of chemical signals. However, the manner in which such information is integrated to implement algorithms for navigation remains obscure (55). For comparison, in the visual system, motion detection is accomplished by integrating several cues over time and specific algorithms have been proposed for how this is done (56). Such a level of description for odor-guided navigation is still being developed (57). Very different physical constraints are imposed on navigation strategies at the different scales and distances involved. Nearly all algorithmic prescriptions offered to date for navigation rely on calculating local temporal or spatial gradients in concentrations (57–63), and apply only to tracking at very short distances, as elaborated below (some exceptions include Reference 64). Accordingly, circuit analysis has tended to focus on how asymmetries in activation of the two olfactory sensors, mimicking spatial gradients, are coded in the brain (65–67).

3. WHAT IS THERE TO BE SENSED? SPATIOTEMPORAL INFORMATION IN AN AIRBORNE ODOR SIGNAL

As an animal navigates a natural environment in search of relevant odor sources, such as food or mates, the perceived odor signal conveys information about the external olfactory landscape. The

signal that reaches the nose or antenna is a fluctuating time series, $\mathbf{c}(t)$, that mixes odors from sources in the animal's surroundings, which are often many and unknown. An odor-guided animal is thus faced with two challenging tasks: separating out and identifying behaviorally relevant sources from a complex background, and inferring the location of a distant source for navigation.

Source–background segregation: the ability to efficiently detect specific odorants of interest against variable backgrounds

Nonadditive mixture response: a nonadditive response to odor mixtures, which is required to prevent saturation and enable source–background segregation

For the former, the animal is required to accomplish source–background segregation, that is, decompose the time series $\mathbf{c}(t)$ as the sum of source and background signals: $\mathbf{c}(t) = \mathbf{c}_s(t) + \mathbf{c}_b(t)$. The task has been termed the olfactory cocktail party problem (68), analogous to the auditory task of focusing on specific auditory signals among a noisy background (69). When the background is constant, neural mechanisms for habituation (70, 71) effectively subtract out the background stimulus, thereby allowing fine discrimination between odors as well as the identification of novel ones. Alternative strategies are required when the background fluctuates strongly in concentration and composition, which is the norm in natural environments. If the source and background are physically well separated, the fluctuations in the turbulent flow that carries these signals are independent. This independence in the temporal statistics of $\mathbf{c}_s(t)$ and $\mathbf{c}_b(t)$ can then be exploited for source separation (72). Instead, when the source and background covary, the signal received is a well-mixed blend, which is to be segregated by the olfactory sensory apparatus. In this case, a strong background can fully suppress perception of the source, a well-characterized phenomenon from olfactory psychophysics known as overshadowing (73, 74).

Effective source separation on a complex background requires a nonadditive sensory response to odors. To illustrate the reason, consider a simplified scenario in which each odor binds and activates a certain subset, constituting a fraction p of all receptor types that can be ON or OFF. Experimental estimates place this fraction p at 10–20%, reflecting the promiscuous binding of ORs (75–77). Note that humans and mice have approximately 400 and 1,000 receptor types, respectively, which enables a combinatorial code for odor identification. When K odors are present in the environment, each of these K odors binds to a different subset of p receptor types. If receptor binding and activation were additive, each receptor would act as a logical OR gate so that the fraction of active receptors is $1 - (1 - p)^K$. If the background has many odor components ($K \geq 10$), additive processing would imply that the sensory apparatus saturates exponentially with K, conveying no information about the source to higher-order processing centers in the brain.

In reality, a series of recent experiments show that odors compete for receptor binding and display a wide range of binding and activation efficacies (28–33, 78). This implies a nonadditive mixture response, where an odor that binds strongly but activates a receptor weakly can competitively antagonize another potent odor that binds weakly to the same receptor. At the ensemble level, antagonism preserves information about subdominant sources of odors by ensuring that the receptor ensemble is not saturated. This is because the activity of the receptors that an odor binds weakly gets modulated by other components in a complex mixture. By contrast, the receptors that the odor binds strongly retain their activity. The combinatorial nature of odor coding then implies that a few highly sensitive receptors are sufficient to uniquely identify an odor, for example, using primacy coding (38). Theoretical models that incorporate antagonism show that source–background segregation is possible even with $K \geq 50$ fluctuating components in the background (28).

Although the above sensory processing mechanisms can enable source identification, information about source concentration is still lost because of the presence of the background. Inhibition of odor intensity by other odors is indeed commonly observed in psychophysical experiments (74). For instance, when two odors of equal perceived intensity are mixed, then the perceived intensity of each component is equally suppressed, an effect known as reciprocal suppression. Although higher-order cognitive processing (79) may play a role in these effects, they are also consistent with the nonadditive, antagonism-mediated mixture processing at the receptor level described above.

However, strong fluctuations in odor concentration imply that precise concentration estimates, beyond the presence or absence of a signal, have little information about source location and, thus, do not offer a great advantage during an olfactory search, as discussed in more detail below.

Spatiotemporal aspects of the source signal $\mathbf{c}_s(t)$ yield information about where the source is located and, consequently, guide an olfactory search. Different locations downwind of the source exhibit different temporal statistics, depending on the statistical aspects of the turbulent flow in any particular environmental condition. Identifying the crosswind position of the source is a central aspect of an airborne olfactory search. If the crosswind position is known, the animal can orient upwind and move directly up the wind axis to reach the source. The symmetry of the signal statistics around the downwind axis implies that it is impossible to resolve the crosswind position using a single stationary sensor. A searching animal is of course not stationary and collects cues while simultaneously navigating its environment. An efficient searcher can move and actively dictate how subsequent information is gathered at spatially separated locations.

Active exploration is in fact a necessity in the dilute regime of sparse odor detections. As discussed below in Section 4.4, turbulent transport makes the detection statistics intermittent; i.e., intervals of odor concentration above the detection threshold, t_w (whiffs), cluster and are separated by long intervals beneath the threshold, t_b (blanks). This is apparent in the experimental concentration trace shown in **Figure 3**. Specifically, the distribution of intervals between consecutive whiffs (i.e., $t_u = t_w + t_b$) exhibits a $-3/2$ power-law scaling regime cutoff at small and large timescales by τ and T_u, respectively: $p(t_u) \sim t_u^{-3/2} e^{-\tau/t_u - t_u/T_u}$ (80). The mean duration between whiffs is then $\langle t_u \rangle \propto \sqrt{\tau T_u}$. The power law implies that most fluctuations in the odor signal contain little information about location; relevant information instead comes from intervals comparable with the upper cutoff T_u, which depends on the source's location relative to the searcher. However, the upper cutoff grows, and consequently, the rate of information declines with downwind and crosswind distance (80). It is therefore advantageous to forage for a signal rather than remain stationary and run the risk of extremely long waiting times before any signal is found.

In a single instant, spatially separated samples can be obtained by comparing the odor signal across nostrils or antennae; this is the analog of visual and auditory stereo-sensing used for depth perception and sound localization, respectively. When the animal is close to the source and the signal is relatively smooth, stereo-sensing may indeed yield instantaneous directional information useful for tropotaxis (2, 59, 65, 66). However, as detailed below, the paths taken by air packets are not straight nor smooth and the advantages of olfactory stereo-sensing further away from the source are less clear. In this case, a simple difference in the signal across the two sensors is extremely noisy and merely reflects fluctuations in turbulent mixing. Nevertheless, the distribution of whiff intervals for the two sensors depends, as in the one sensor case, on the paths taken by the air packets that reach these two sensors and should thus retain some usable spatial information if the sensors are distant. Whether this information can be fruitfully decoded and used within the sensorimotor and physical constraints of an olfactory search remains an open question.

4. HOW ARE ODORS TRANSPORTED BY ENVIRONMENTAL (TURBULENT) FLOWS?

The equivalent of the Reynolds number (82) for the transport of particles, such as odorants, is the Péclet number: $\mathrm{Pe} = \frac{uL}{\kappa}$, where u and L are the characteristic velocity and length-scale of the flow transporting the particles, and κ is the molecular diffusivity of the transported particles. As for Reynolds numbers, low Pe transport is dominated by molecular effects, whereas high Pe corresponds to turbulent transport (with a slight abuse of language as trajectories of particles can be chaotic and mixing even for nonturbulent flow; 83, 84).

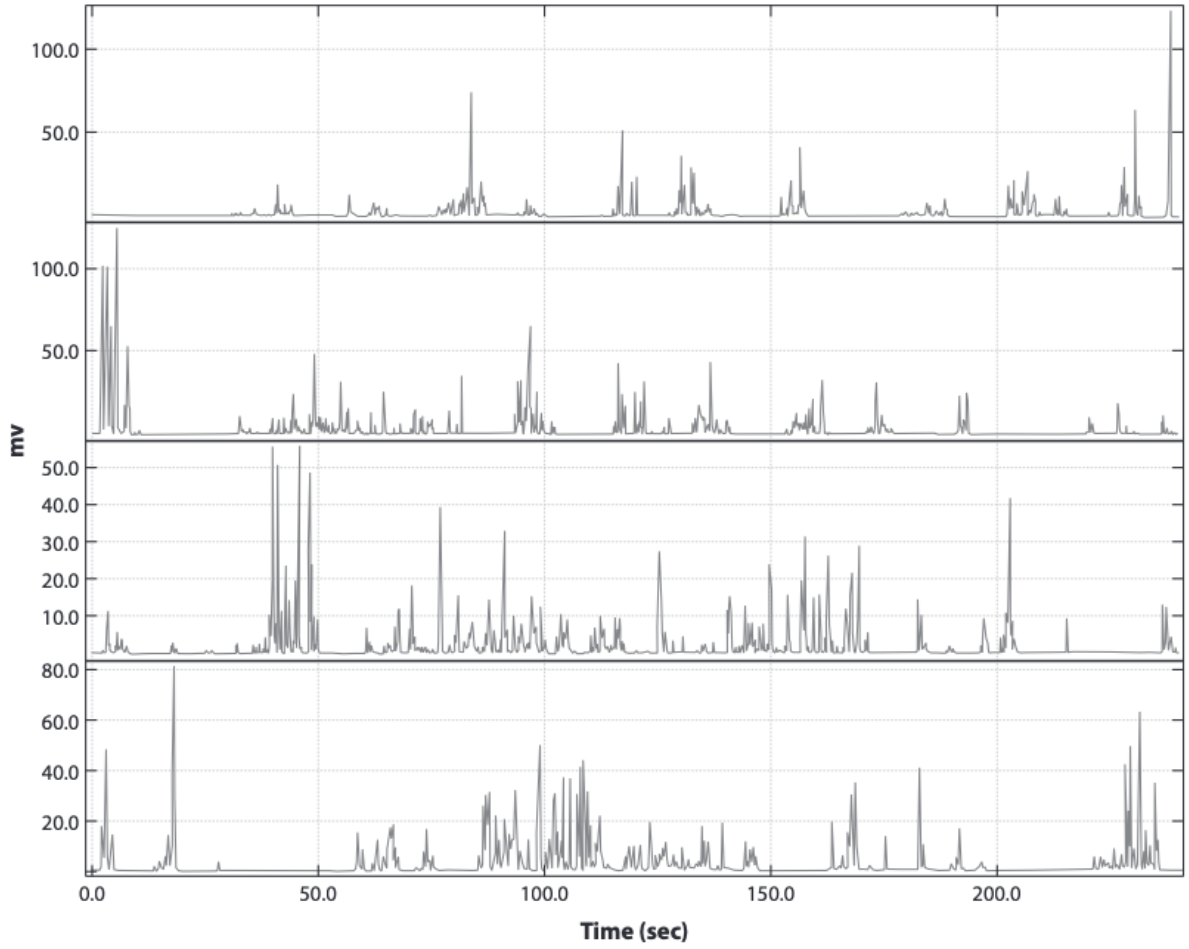

Figure 3

A concentration time series of duration 16 min (the *y* axis reports the raw signal from the detector): Data are continuous from the top panel to the bottom one, with each panel exhibiting 4 min of data. The time series was measured on the mean-plume centerline at a distance of 50 m from a source of propylene placed at a height of 2.5 m above the ground under near-neutral stability conditions. The graphs provide a vivid illustration of intermittency and clustering of odor detections at long distances from a source, with periods of no detection that can last tens of seconds. Figure adapted with permission from Reference 81.

4.1. Turbulent Transport Is More Effective than Its Molecular Counterpart at Dispersing Particles

The classical G.I. Taylor's analysis (85) considers the displacement of particles moving along Lagrangian trajectories $X(t)$ defined by the equation $\frac{dX(t)}{dt} = U[X(t), t]$, where $U = V + \tilde{v}$ is the transporting velocity decomposed into its mean V and fluctuating component $\tilde{v}$. The former advects particles as a whole, whereas the latter disperses them. Squaring the fluctuating component of the displacement $X(t) - X(0)$, averaging over the statistics of the flow, and assuming stationarity (and time-symmetry for simplicity) of the Lagrangian covariance function $C(|s - s'|) = \langle \tilde{v}[X(s), s]\, \tilde{v}[X(s'), s'] \rangle$, one obtains Taylor's formula:

$$\langle [\boldsymbol{X}(t) - \boldsymbol{X}(0)]^2 \rangle = 2t \int_0^t C(s)\, ds. \qquad 1.$$

At times $t \ll \tau \equiv \int_0^\infty C(s)\, ds / C(0)$, the Lagrangian correlation, $C(t) \simeq C(0) = \langle \tilde{v}^2 \rangle \equiv v^2$, and ballistic motion, $\propto t^2$, ensues. The behavior at intermediate times depends on the flow and leads to the anomalous scaling laws discussed in Section 4.3. Finally, at $t \gg \tau$, scale separation holds, and

one obtains the Gaussian diffusive behavior $2Dt$ (85). The expression for the effective diffusivity $D = \int_0^\infty C(s)\,\mathrm{d}s = v^2\tau$ is also estimated as $v\lambda$, where the characteristic length $\lambda = v\tau$. We see then that the ratio defining the Péclet number is itself the ratio between turbulent and molecular diffusivities.

Let us now contrast molecular and turbulent transport. Particles of a gas (or a liquid) move at speeds greater than the speed of sound, yet their collisions reach frequencies of 10^9–10^{10}/s, limiting their mean free path λ to an order of magnitude O (100 nm). Conversely, olfactory turbulent flows are well subsonic, yet their typical scales are macroscopic. Typical numbers for laboratory experiments on odors are $U \sim O$ (m/s) and $\lambda \sim O$ (m), and they are even larger in the field. Inserting these estimates into the above expression for D, it is clear that the molecular diffusivity is several orders of magnitude smaller than its turbulent counterpart. That is why odors would take forever to be dispersed in the absence of turbulence. Another consequence is that ratios among constituents of a blend of molecules are largely preserved during the transport of mixtures by a turbulent flow. The only exceptions to molecular diffusion being negligible are at very short distances to a source of odors and close to a surface, where thin boundary layers and/or adsorption processes are important.

4.2. Turbulent Transport Is More than Enhanced Diffusion

Turbulence generates snapshots of concentration fields that differ fundamentally from those generated by diffusion, as illustrated in **Figure 1** and shown by dyes injected in a water jet in **Figure 4**. To grasp the underlying physics, it is instructive to contrast environmental air-quality problems and olfaction studies, both of which investigate turbulent transport. A typical situation considered by the former is the dynamics of plumes emitted from industrial stacks and their impact upon the quality of air, health, and human welfare. Long-term effects (on scales of several days and longer) are, therefore, relevant (86). Conversely, olfactory searches typically take place over minutes, and the behavioral response times of various animals can be as fast as hundreds of milliseconds (40, 42, 87). On long environmental timescales, Taylor's formula (Equation 1) reaches its asymptotic regime, and effective turbulent diffusivities are relevant, as in Sutton's plume model (88). That is not the case for olfactory studies, in which behavioral times are too short; this is also shown by direct measurements (89, 90).

In summary, scale separation does not usually hold for the transport of odors; i.e., their relevant length- and timescales are within the broad range of scales typically excited in natural turbulent flow. Two major consequences for olfaction are discussed next.

4.3. Scaling Laws in the Evolution of Particle Dynamics

In the absence of scale separation, the integral in Taylor's formula (Equation 1) keeps changing, which can lead to power-law behaviors across the broad range of scales typical of turbulent flow (92). Indeed, a scale-invariant correlation function C can yield a $t^{2\alpha}$ behavior with an exponent $\alpha \neq 1/2$, leading to anomalous diffusion (93). In particular, $\alpha = 1$ reflects ballistic transport, which is often observed at times shorter than decorrelation times.

For instance, typical parameters (94) for a jet flow, as shown in **Figure 4**, are as follows: The mean velocity is $V \sim 0.6$ m/s, and the flow decorrelates on a timescale of $\sim L/v$, where the root-mean-square (rms) turbulent velocity is $v \sim 20\%$ of the mean V and the characteristic length defined by the jet geometry is $L \sim 6$ cm. The downstream decorrelation length VL/v is then $\sim$30 cm, which is several times greater than the longest distance to the source where measurements are made. It follows that, in each realization of the flow, a particle is effectively transported by a

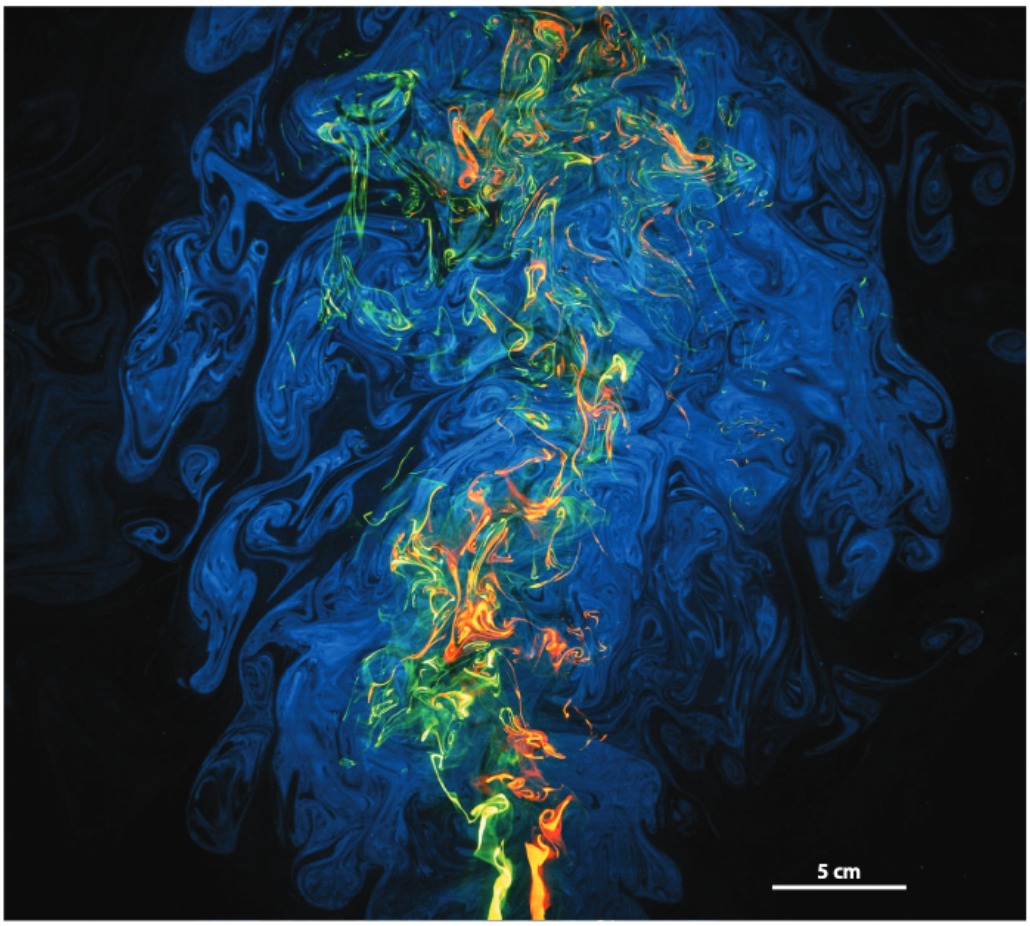

Figure 4

Two separate sources of fluorescein (*green*) and rhodamine (*red*) are injected on the axis of a turbulent water jet (*blue*), in its downstream far field. The image shows a two-dimensional cut through the two instantaneous concentration fields, which illustrates the complexity of concentration fields generated by turbulent transport as compared with those generated by diffusive processes. Figure adapted from Reference 91 with permission of AIP Publishing.

frozen snapshot of the flow with spatial fluctuations of rms amplitude v. These fluctuations induce a lateral dispersion that grows in time as vt. Because particles progress downstream as $x \sim Vt$, the plume has a conical shape of angular aperture v/V. Similar arguments (80) hold for a conical shape in the neutral atmospheric boundary layer. Note that the above scaling crosses over to different scaling laws at smaller and larger downstream distances. This is a common feature in turbulent transport: General scaling laws are often observed, yet their ranges and transitions depend on the flow and require specific analysis.

Scaling laws are important because they control the dispersion of particles and, therefore, their dilution rate in space and time. A key quantity is the width $r(x)$ of the average turbulent plume, at distance x downwind from the source. The width delineates the region in which it is likely to find a substantial concentration of the substance. Conservation of mass implies that the typical concentration $c(x)$ within the plume satisfies the flux-balance relation $J = c(x)r(x)^2V$, where V is the magnitude of the mean wind, and the emission rate in molecules per unit time is $J \sim c_0a^2V$, where c_0 is the concentration at the source and a is its size. The mass conservation relation combined with the animal's detection threshold c_{thr} determines the detection range x_{thr} by the relation $r(x_{\text{thr}}) = a\sqrt{\frac{c_0}{c_{\text{thr}}}}$. As noted in Section 4.3, the average plume is conical in a jet and in the neutral atmospheric

boundary layer, and $r(x) \sim \frac{vx}{V}$, where v is the rms velocity. Let us show how this relation is used to estimate olfactory attraction ranges.

Mosquitoes are attracted by a combination of several human cues, namely human odors and increased levels of CO_2 (95–97). Indeed, the background level of CO_2 in the atmosphere is ~400 ppm, whereas in human breath the level is $c_0 \sim 4\%$. The background level sets the threshold as well as the ratio $c_0/c_{\text{thr}} \sim 100$. Given a source of size $a \sim 1$ ft and a typical angular aperture of the cone (turbulence level) $v/V \sim 20$–30%, we obtain an estimate of $x_{\text{thr}} \sim 15$–20 m, which is consistent with field observations of mosquitoes baited by a CO_2 source (98).

4.4. Lagrangian Dynamics, Intermittency, and Clustering of Odor Detections

Even within the average turbulent plume considered in the previous section, the pattern of detections drastically differs from continuous profiles typical of diffusive processes. **Figure 3** shows data for typical long-distance profiles of odor detections, which witness the broken nature of odor plumes sketched in **Figure 1*c***. The salient feature is the strong intermittency, i.e., the presence of clusters of time intervals with odor concentration above the detection threshold (whiffs) separated by intervals beneath the threshold (blanks) that can last for tens of seconds. Consequently, unless the animal is very close to the source, concentration averages over short periods of time are noisy and unreliable indicators of source location.

The physical origin of intermittency is intuited by tracing back the ensemble of paths taken by an air packet before it arrives at the olfactory sensor at a given time. These Lagrangian paths meander because of turbulent fluctuations and charge odor when they overlap with odor sources, as mathematically expressed by the passive scalar (99–102) equation: $\partial_t c + (\boldsymbol{V} + \boldsymbol{v}) \cdot \nabla c = \kappa \Delta c + J$. Here, the scalar field $c(\boldsymbol{x}, t)$, e.g., odor concentration, is transported by a mean $\boldsymbol{V}(t)$ and a fluctuating $\boldsymbol{v}(\boldsymbol{x}, t)$ velocity field, and is injected by a source (spatially localized over a region of size a) at a rate J. The diffusivity κ accounts for molecular noise, and we neglected, for simplicity, inertial effects (see References 103, 104). In terms of (noisy) Lagrangian trajectories, the above equation states that the field is conserved unless the trajectory overlaps with the source (101).

The Lagrangian framework turns the issue of scalar statistics into a residence-time problem, which is more intuitive. For instance, the long blank intervals in **Figure 3** correspond to situations in which the air packet does not overlap at all with the source, which can be quite common especially out of the wind axis. Once wind fluctuations push the ensemble of paths away from the source, temporal correlations make these fluctuations persist and lead to long intervals of no odor detection until the ensemble of paths reintersects with the source. Clustering is also intuitive as air packets at relatively close times experience similar velocity realizations along their paths; therefore, the air packets have highly correlated chances of overlapping with the source. The combinations of these dynamical processes are the physical basis for intermittency, sporadicity, and clustering of odor detections. For further details and the derivation of the $-3/2$ scaling law for the distribution of whiffs and blanks discussed in Section 3, we refer to Reference 80, where field data for smooth and flat grounds are also discussed (105). The presence of a canopy or inhomogeneities in the landscape can lead to additional large-scale fluctuations and/or modulations of the wind structure (90) that sweep odor packets off the source and, therefore, impact the cutoffs for whiffs and blanks.

5. NAVIGATIONAL STRATEGIES

Navigational strategies greatly influence the survival of an olfactory animal and encompass the full complexity of decision-making under uncertainty. Lessons learned from dissecting strategies employed by animals directly inspire biomimetic applications (106), whereas computational studies

using ideas from machine learning provide insight into the constraints faced by animals. The wide range of possible scenarios that an animal could face in a natural environment combined with the stochasticity of turbulent transport indicates that olfactory navigation is a challenging task. Yet, consistent patterns are observed across species and reproduced in computational studies, hinting that certain general principles underlie effective navigation. First, gradient climbing is very effective in the presence of smooth concentration fields, and a variety of sensorimotor strategies are observed in nature to estimate gradients whenever continuous cues are available (Section 5.1). We have kept Section 5.1 brief for two reasons: (*a*) Our focus is on turbulent environments, where continuous cues are typically not available, and (*b*) numerous reviews and articles on gradient climbing are present in the literature, as detailed in Section 5.1. Second, surface-bound odor trails typically provide continuous cues as the animal keeps close contact with the trail (Section 5.2). However, odor detections can become sporadic if the animal often loses the trail, for instance, because of breaks or sharp turns, which leads to wide lateral excursions with respect to the trail path (casting). Finally, casts across the wind alternated with upwind surges are also a recurrent pattern for insects flying in a turbulent environment (Section 5.3). Although reactive strategies can qualitatively reproduce these patterns, the same holds true for qualitatively distinct, model-based strategies that rely on learning on the fly (Section 5.4). This dichotomy motivates the need for further and more specific experiments addressed in Section 6 titled Future Challenges.

5.1. Chemotactic Gradient-Climbing of Smooth Concentration Fields

The definition of chemotaxis is the oriented locomotion (taxis) of cells or organisms in response to a chemical stimulus. In practice, research has historically focused on the motion of microorganisms, and the term chemotaxis now commonly refers to mechanisms that allow navigation in the presence of well-defined gradients of chemicals, as is the case in the microscopic world. The paradigm among bacteria is the run-and-tumble motion of *Escherichia coli*, which climbs (or descends) gradients by estimating concentration gradients across time and regulates its frequency of tumbling accordingly (107). The size of the cell or organism critically influences the physical constraints on sensing and directed locomotion (108). For larger cells, spatial gradients can be estimated by measuring concentration differences across the cell body, as in the slime mold *Dictyostelium discoideum* (109, 110). Other unicellular organisms and small animals use a variety of modalities to achieve the same functional goal of estimating gradients of concentration in the neighborhood of the organism and informing reorientations. For instance, alternation of lateral movements of physically localized sensors, e.g., on the head of the animal, or stereo-sensing at physically separated sensors, like two antennae, generates a comparison between different directions (111–118). Gradient climbing can be employed for airborne odor navigation when the animal is close to the source (5). The gradient-climbing paradigm is so intuitive (and successful in the microscopic world) that similar ideas are often proposed even in conditions in which gradients are not available.

5.2. Tracking of Surface-Bound Odor Trails by Terrestrial Animals

Although trail tracking behavior, especially by dogs, is a familiar phenomenon, the corresponding search strategies remain poorly understood. Surface-borne odor trail tracking imposes a different set of geometric constraints compared to airborne cues though certain aspects of behavior are similar, as discussed below. Adsorbed scent establishes a long-lasting trace compared to transient fluctuations in an airborne signal. This is exploited by trail tracking animals to hunt and forage. Forensic studies of well-trained trailing dogs provide ample evidence of an astounding trail

tracking capacity: In one study, experienced bloodhounds successfully tracked 96% of two-day-old human scent trails ranging from 0.5 to 1.5 mi within urban environments (119). Similar case studies highlight bloodhounds' abilities to identify and follow weeks-old scent trails for kilometer-range distances. In dogs, an initial foraging phase to find the trail is followed by a determination of the trail's directionality and subsequent tracking (120–122). Behavioral algorithms underlying these various phases remain unknown.

Other animals that excel at trail tracking are ants and rodents, which are more amenable for lab experiments. Although the sensorimotor constraints across animals differ, the basic features of the task are retained. In particular, trail tracking involves following a broken or continuous, meandering line trail. Regardless of how information is obtained and integrated, any trail tracking strategy should involve continuous, feedback-based reorientation of the animal along the general direction of the trail. Rats on a treadmill are able to track odor trails efficiently in the dark, often staying in close contact with the trail (3). The trajectory of the rat resembles a small-amplitude zigzag around the trail, which switches to a large-amplitude oscillatory casting motion when the trail is abruptly broken. Carpenter ants either employ a crisscross sampling strategy using their antennae or execute a sinusoidal motion around the trail (15).

On the theoretical side, a class of models proposed to rationalize the above behaviors rely on variants of chemotaxis (3, 4, 58). For instance, one such strategy has the animal turn to the opposite direction if it experiences a significantly declining odor gradient along its trajectory. However, rats with a blocked nostril and ants with a single antenna are still able to track trails, although less accurately (3, 15). Furthermore, though chemotaxis-based strategies may allow for trail tracking when trails are continuous, they fail when trails are broken and gradients are absent, which is certainly relevant for animals tracking trails in the wild. These fundamental limitations motivated a recent alternative to chemotaxis that is based on the intuitive idea that the trail's heading can be utilized to orient along the trail (123). The trail's heading and its uncertainty, which are estimated using the animal's past contacts, delineate the angular sector in which the trail is likely to head. The analysis of the resulting sector search leads to a series of predictions about the speed and geometry of the search that are consistent with existing data and suggest a range of new experimental tests.

In conclusion, trail tracking is a familiar behavior and offers a novel paradigm to examine the computational principles behind odor-driven navigation. Many key questions remain open, reflecting the dichotomy between reactive strategies versus learning during navigation: Do animals retain a memory of past contacts? If they do, how much and what internal model do they use to integrate this past information? Do animals actively learn the statistics of a trail and modulate their strategy and speed accordingly? When do animals give up tracking and transition to other behaviors (such as foraging or turning back), having decided that the trail is lost? Future experiments with ants or rodents, along with the developing tools for automated behavioral tracking, are expected to bring rapid progress on all these questions.

5.3. Insect Navigational Strategies

For flying insects, olfaction is the primary means of communication, and effective olfactory navigation dictates their survival (99, 124–126). A salient example is the pheromone search of a male moth for a female (127, 128), as illustrated in **Figure 5**. Numerous studies have examined this phenomenon, both in the field and via wind tunnels. Estimates of the range of pheromone communication are between tens of meters and a kilometer, depending on the moth species (129). Search patterns in moths and other insects are indicative of an ability to orient upwind and that this capability is necessary for navigation. This is achieved through a mechanism known as

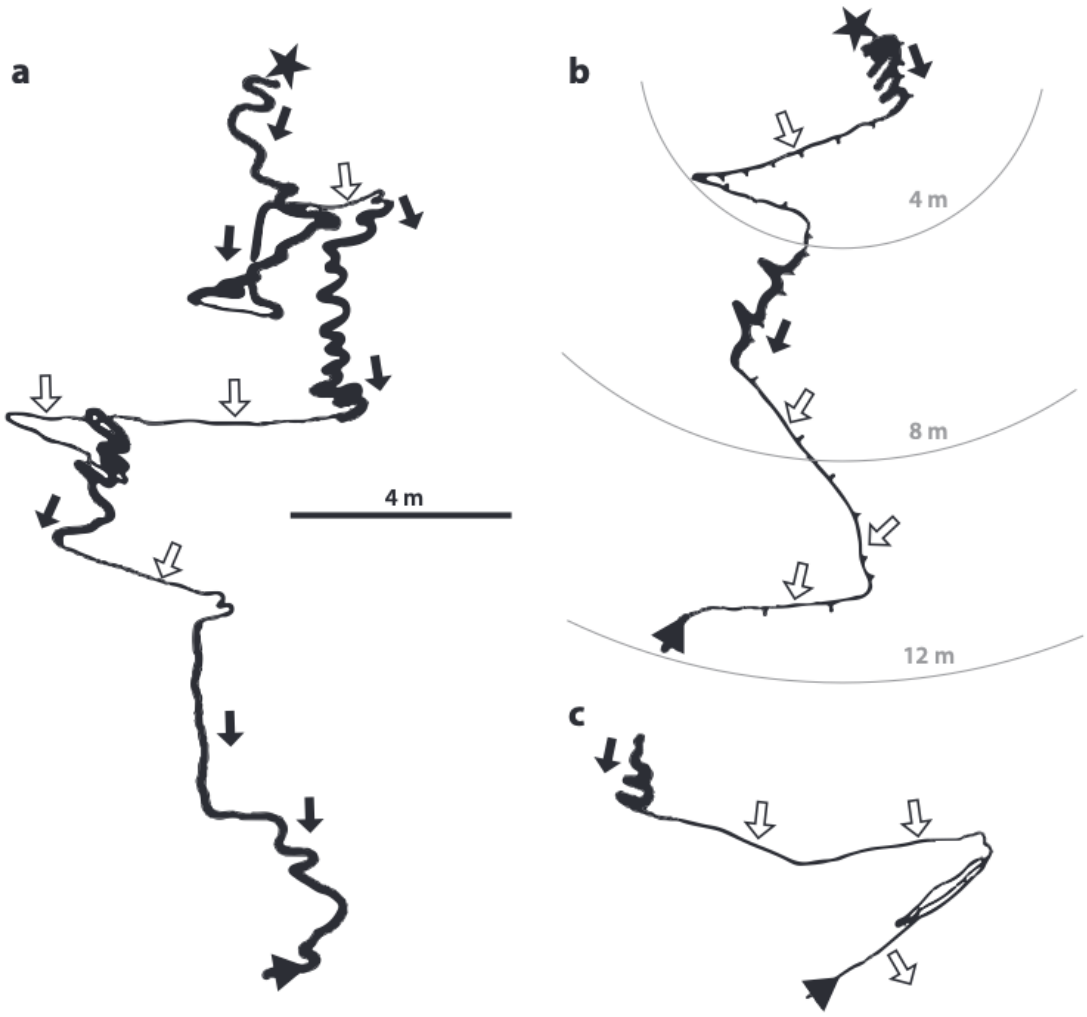

Figure 5

Tracks of male gypsy moths approaching a source releasing sex pheromone together with bubbles (that can be visualized and provide a sense of the distribution of odor stimuli) (127). Panels *a* and *b* show two typical tracks, with thick/thin parts referring to periods within/outside the bubbles, i.e., likely associated with high-frequency/absence of odor detection. Thick parts are known as surge, as they show consistent progression up the wind (indicated by arrows). Conversely, thin lines show crosswind motion and are known as casting. The portion of a track in panel *c* shows that a change in wind direction is reflected in the orientation of behavioral moves. Figure adapted with permission from Reference 127.

optomotor anemotaxis (130), where the insect reorients itself so as to minimize side slip in its optic flow. Within a pheromone plume, the search patterns of a moth consist of a surge or a zigzagging upwind motion around the wind axis. The zigzagging is generated via a strikingly robust, periodic counter-turning behavior with 3–5 reversals per second across a variety of conditions. This robustness persists across species, suggesting a common motor program underlying these patterns. Upon sustained loss of contact, casting is observed, in which the insect executes wide, crosswind excursions of increasing amplitude. Casting likely reflects a foraging strategy, employed to maximize the probability of reencountering the plume. The statistics of the stimuli (or the lack of them) that trigger and modulate casting in different conditions remain unclear, primarily owing to the difficulty of measuring precisely when the insect encounters or loses contact with the plume. These measurement challenges are partly circumvented in wind tunnels that use a controlled, laminar stimulus. However, a pulsed odor ribbon at a high frequency triggers a

qualitatively different behavior and a more efficient search compared to a stable odor plume, suggesting that odor statistics are critical to reproduce field behavior (40, 131). The weaving of an insect in and out of a stable odor ribbon has been used as a proxy for turbulent intermittency, under the assumption that the memory of past encounters with the plume is smaller than the time spent between encounters. Experiments using this methodology and automated tracking systems show that the fruit fly *Drosophila melanogaster* exhibits a qualitatively similar surge-and-cast pattern as the moths, hinting at a conserved strategy that effectively deals with the constraints imposed by turbulence (132, 133). Still, beyond broad similarities, some differences remain within and across insect species. For example, fruit flies execute a continuous surge within the plume, whereas moths may cast even within a homogeneous plume. Whether these differences reflect distinct olfactory sensory pathways or motor programs is unclear. An enduring challenge is the simultaneous tracking of flying insects and control of the stimulus experienced by the insect under realistic flow conditions.

Surge-and-cast: a surge is a brief upwind movement while casting is a sequence of crosswind excursions of increasing amplitude

Like flying insects, walking insects display anemotaxis-driven navigation toward an attractive odor. Walking insects offer a window to examine odor-evoked responses with lower Reynolds number environments, smaller arenas, and better control of stimuli. Responses are driven by modulation in the turning rate, the stopping probability, and the rate of locomotion along or across the wind axis. Experiments with cockroaches recapitulate the observation that plume statistics strongly influence behavioral trajectories, with wider plumes generating wider amplitude crosswind excursions and more frequent stops (134, 135). The search efficiency of cockroaches depends primarily on the total antennal length irrespective of their having one or two antennae, hinting at a minor role of tropotaxis. Fruit flies in a fluctuating plume increase upwind velocity and turn probability with an approximately linear response to the onset and offset of the odor stimulus (136). Using smoke as an attractant, the plume can be visualized while tracking the movement of the flies, which allows for an analysis of the response triggered by a series of discrete odor encounters (137). In this experiment, fly response is best explained by the frequency of odor encounters, where flies increase their upwind turning bias based on the frequency of odor encounters and the rate of stopping transiently increases after an encounter. Questions related to conditioning and reward-based modulation of responses remain open. As in the case of surface-borne trail tracking, whether insects can adapt to the statistics of the environment and whether this can account for differences of behaviors in References 136 and 137 is unknown. Finally, how insects integrate odor, visual, and mechanosensory cues in diverse environments, particularly for the final stage of reaching the source during olfactory navigation, remains largely unexplored (see References 138 and 139 for two notable exceptions).

5.4. Model-Based Strategies: Infotaxis and Partially Observable Markov Decision Processes

The infotaxis strategy (140) was introduced to address long-distance navigation, where gradients of concentration are not reliable. To overcome the scarcity of detections and the resulting sparsity of information about the location of the source, the strategy maintains an estimate of the location of the source relative to the searcher x. The agent moves to maximize the expected rate of information gain about x based on observed cues o (the detection or absence of an odor signal or the discovery of the source) and a model $\Pr(o|x)$ that incorporates odor transport. The location x is a latent state; i.e., the exact state is unknown but is maintained as a "belief" or posterior distribution, $\Pr(x) \equiv \boldsymbol{b}(x)$. Accounting for the transitions due to actions, the full Bayesian update of the prior belief vector $\boldsymbol{b}$ on taking an action a and observing o is $\boldsymbol{b}^{o,a}(x) \equiv \Pr(x|o,a,\boldsymbol{b}) \propto \Pr(o|x,a) \sum_{x'} \Pr(x|x',a)\boldsymbol{b}(x')$. The infotaxis policy given the current

belief is

$$\pi_{\text{infotaxis}}(\boldsymbol{b}) = \arg\max_{a} \left\{ \sum_{o,x} \Pr(o|x,a)\boldsymbol{b}(x) \left[H(\boldsymbol{b}) - H(\boldsymbol{b}^{o,a}) \right] \right\}, \quad 2.$$

Exploration and exploitation trade-off: the trade-off central to decision making under uncertainty, which captures the balance between gathering information and exploiting existing knowledge

where $H(\boldsymbol{b})$ is the Shannon entropy of $\boldsymbol{b}$. Equation 2 captures the two sides of the exploration and exploitation trade-off. The possibility that the source could be found at a nearby location, which leads to a complete loss of entropy $H(\boldsymbol{b})$, drives greedy exploitation. The other factor driving the search is the expected loss of entropy by potential odor cues found through efficient exploration (140). Infotaxis has been applied on numerical simulations and experimental data and implemented in olfactory robots for the automated detection of chemical and toxic leaks as well as explosives (141, 142). Results demonstrate that the source can be located despite the absence of gradients, and the zigzagging-casting pattern observed in animals is conserved in realistic environments. The infotaxis principle can be generalized to a swarm of agents (143, 144): Individuals maximize their information acquisition and minimize overlap with other individuals, which leads to substantial gains compared to independent random searchers (145).

Optimality of infotaxis (as in other applications of information-acquisition principles; 146–149) is open. A continuous-space version was formulated to that aim in Reference 150, but the real bottleneck is the coupling between the agent's strategy and the statistics of odor detections. When this coupling is absent, e.g., in multiarmed bandits, acquisition of information is provably optimal (151). At shorter distances to the source (when lack of information is not limiting), shifting the balance toward exploitation is expected to be more effective, as also demonstrated by the free energy formulation in Reference 142. This work also confirmed that the principle introduced in Reference 140 is not restricted to its original implementation, *viz.*, coarse-grained maps with a handful of parameters and simple updates for the entropy suffice to drive the agent to the source. Claims that memory and calculations of infotaxis are appropriate for robots only are, therefore, not justified, and simplified forms of information acquisition may be relevant for animals. Learning components beyond purely reactive strategies have indeed been evidenced in the behavior of fruit flies and mosquitoes (152), silk moths (153), and *Caenorhabditis elegans* (154).

Infotaxis is related to a broader learning framework known as partially observable Markov decision processes (POMDPs), which offers the flexibility to build normative models of decision-making under uncertainty across a wide range of conditions. POMDPs generalize Markov decision processes (MDPs) for modeling decision-making by an agent operating in a stochastic environment influenced by its actions (155, 156). In MDPs, transitions between states depend on the current state (Markov property) and actions taken by the agent (generalizing Markov processes to MDPs) at each step. On executing the action, the agent is given a reward. The goal is to find optimal policies, which pick actions that maximize the expected (discounted) sum of future rewards, which is also called the value function. POMDPs generalize the MDP setting to the case in which the system has only partial information about its current state.

The basis for most learning algorithms in MDPs and POMDPs alike is the Bellman equation—which is a recursive self-consistent equation for the value function V of the various states (157). The Bellman equation for POMDPs reads as follows:

$$V(\boldsymbol{b}) = \max_{a} \left\{ E_{\boldsymbol{b},a}(r) + \gamma \sum_{o,x} \Pr(o|x,a)\boldsymbol{b}(x)V(\boldsymbol{b}^{o,a}) \right\} \equiv \max_{a} Q(\boldsymbol{b},a), \quad 3.$$

where V is the value function on belief vectors $\boldsymbol{b}$ (instead of fully observed states, as in MDPs; 155), and Q is the action-value function for each action. The POMDP policy is then given by

$$\pi_{\text{POMDP}}(\boldsymbol{b}) = \arg\max_{a} Q(\boldsymbol{b},a). \quad 4.$$

The discount factor γ (in the range of $0 \leq \gamma < 1$) defines an effective horizon $\sim(1-\gamma)^{-1}$, with $\gamma = 0$ corresponding to a greedy policy that maximizes the immediate reward.

Solving a POMDP is challenging as the value function is defined on belief vectors that are high-dimensional (with dimensionality equal to the number of states) and whose components take continuous values between 0 and 1. Exact algorithms exist but do not scale to problems with state spaces of more than ~10 states. Problems with large state spaces, such as olfactory searches, which were previously out of reach, can now be approached using recently developed approximate algorithms to solve POMDPs. These approximate algorithms, particularly point-based value iteration methods, have sped up the process of solving POMDPs, achieving significant gains in problems with up to $\sim 10^4$ states (158). The idea is to find an approximate representation of the value function as a series of hyperplanes. Heuristic methods accelerate the approximation process by improving the value function only at belief vectors that are typically encountered during the process rather than the entire high-dimensional belief vector space. The values at other belief vectors are then extrapolated from the typically encountered ones. A sample trajectory of an olfactory searcher obtained using this approach is shown in **Figure 6** and recapitulates the surge-and-cast behavior exhibited by insects.

6. FUTURE CHALLENGES

Moving forward, a better understanding of the statistics of odors in natural conditions seems important. As discussed in the sidebar titled Why Does the Distance to the Source Matter?, the study of animal behaviors at long distances to natural sources has remained by and large descriptive because of severe technical limitations in experimental methods that could jointly deliver the relevant odors sensed by the animal and its behavioral moves at high-enough resolution. Breaking this deadlock would transform the field in terms of both the relevant features that are extracted by animals and the neural processes that analyze this information to produce appropriate behaviors. Because neural circuits have presumably adapted over evolution to match the environment, testing hypotheses about how the olfactory system extracts features from the odor landscape and providing data on the stimuli–actions associations in natural statistics of chemicals are key to progress.

A second challenge is the development of new behavioral assays in a variety of animals to examine their capabilities and limitations in discerning statistical patterns of natural olfactory stimuli. Recent experiments (87) have hinted that mice, where olfaction is often framed as a low-bandwidth sense, can discriminate signals at frequencies up to 40 Hz. Similarly, insects are known to transduce odors rapidly and track pulses up to 100 Hz (40, 42, 165). How this information can be used in a more deliberative manner (i.e., integration over time) is unclear. Future experiments could explicitly test whether animals can distinguish the mean, variance, and higher-order statistics in the incoming olfactory stimuli and use them to learn about the world for identification and navigation.

The neural mechanisms of how information about fluctuating odors is integrated in the brain to guide navigation are poorly understood. The challenge here is not just characterizing response properties of neurons in various stages, which has tended to be a focus of much technical advance in neuroscience, but also uncovering what the algorithms are. Such explanations require models of how the signals are integrated to form explicit or implicit representations of variables that are used to solve the navigation or tracking problem (166). This endeavor also calls for normative theories of how olfactory searches and navigation can occur rather than ad hoc computational models to fit behavioral or neural data.

Strategies and neural implementation of odor trail tracking are understudied, and the rise of new empirical methods for their study in laboratory settings promises to shed light. The ability

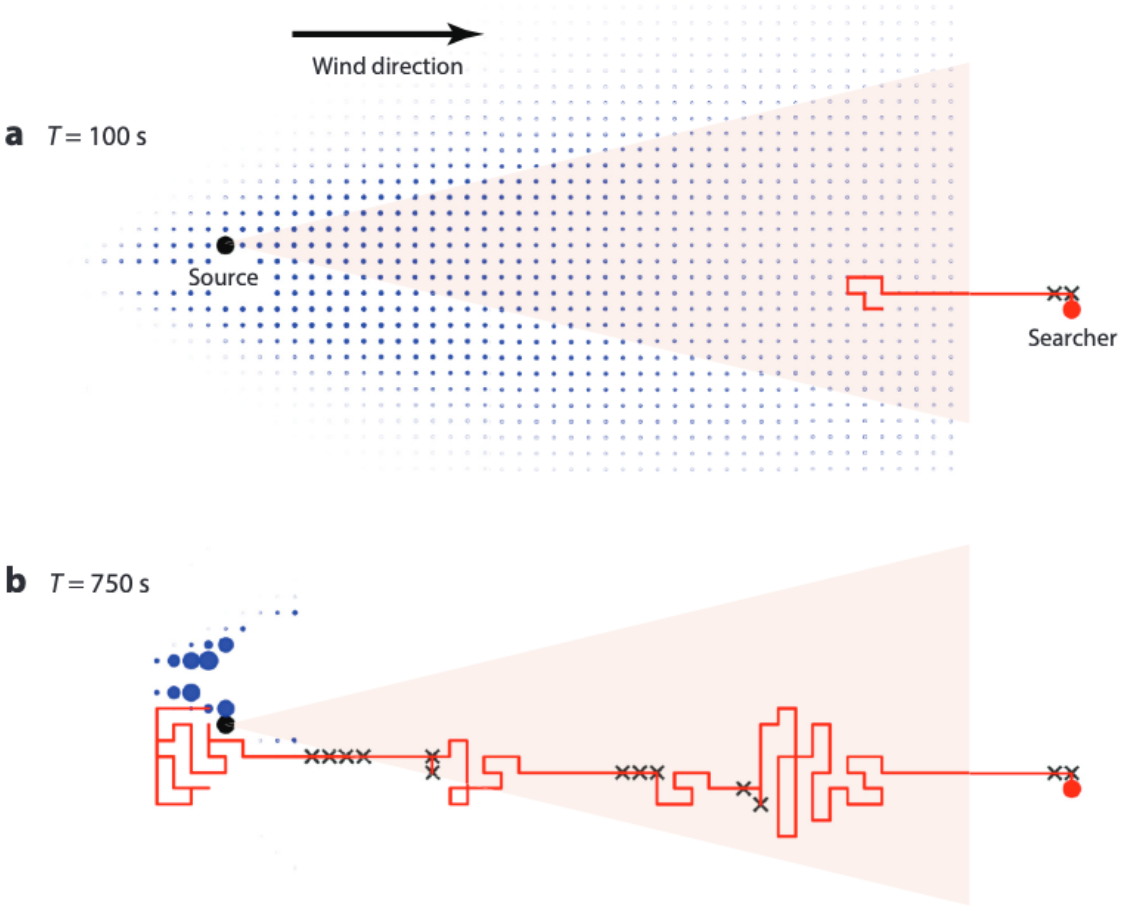

Figure 6

A sample trajectory of a POMDP searcher attempting to locate a source of chemicals that are dispersed by a turbulent environment. Note the sequence of an upwind surge followed by crosswind casts triggered upon a single detection. (*a*) The initial position of the searcher is ~50 units downwind from the source. The darkened area shows the conical average plume with nonzero probability of detecting an odor signal. The size of the blue dots shows the probability of the searcher's location relative to the source, which is initially uniform and transforms to a cone upon the first odor detection (indicated by crosses). (*b*) Close to the source, the searcher exhibits a trial-and-error greedy strategy. Abbreviation: POMDP, partially observable Markov decision process.

to render trails with arbitrary geometry and monitor animals as they track them for long periods of time will aid testing of hypotheses derived from theory (3, 15, 63, 123).

Much of the work done to date has treated odor sensing on the ground and airborne odor sensing separately. However, alternation between sniffing in the air and on the ground by dogs and rodents (3, 5, 120, 122) suggests that ground and airborne cues are exploited jointly. Sniffing in the air can even get to rearing on the hind legs, which is a behavior generally associated with novelty detection and information gathering but can also reflect anxiety and fear (167). Ground and airborne odor signals correspond to different modalities of transport, with ground signals smoother and slower as adsorption processes take place in the boundary layer close to the surface where velocities are reduced, as discussed in Section 4. The puzzle of how animals alternate the two sensory modalities and combine them into a navigation strategy offers fertile ground for future studies.

Natural odor landscapes commonly contain mixtures of smells from multiple sources. The different chemicals from a single source will be well mixed and transported together, as discussed

WHY DOES THE DISTANCE TO THE SOURCE MATTER?

Field studies have demonstrated that long-range searches occur, namely those of male moths searching for pheromones over tens of meters (127), and mosquitoes at ∼20 m to levels of CO_2 emitted by humans (98). However, being in the field hampers the measurement of the olfactory stimulus sensed by the animal. Techniques such as bubbles used in Reference 127 (see **Figure 5**) are ingenious but remain qualitative and do not have the resolution to assay the stimulus-response relationship, which is a central aspect of behavior. These difficulties have limited laboratory investigations to relatively short distances to sources encountered in natural conditions, typically a meter or less. For instance, state-of-the-art work which demonstrates that freely-roaming mice track odors is limited to small arenas (4, 5, 60), where smoothing by time integration allows gradient climbing. Similarly, recent works on insects discussed in Section 5.3 concentrate on relatively short distances: a 1.5-m-long wind tunnel (133, 152), a 3-m-long arena (137), a miniature wind-tunnel setup (136), the plume at 1 m from *Datura wrightii* flowers (43). Information-theoretic analyses on odor encoding were developed for signals at ∼10 cm from the source (159, 160). Finally, neurobiological mechanisms in (161) assume that animals experience on average 14 odor detections along a single cast. This high rate of Poissonian detections (key for orientation) may be appropriate at short distances but long-distance detections along a cast should be clustered and with an average order unity at most (see Section 4.4).

Detailed numbers on distances and frequencies matter because they impact the olfactory signal and the resulting behavior. As sketched in **Figure 1**, at "short" distances, plumes form a meandering trail, which fluctuates and impacts odor encoding (159, 160) but is still continuous, as conveniently visualized in the laboratory (94, 162, 163) (see **Figure 4**). As the distance to the source increases, plumes break up into disconnected patches that feature substantial fluctuations at high frequencies and small spatial scales, and are separated by wider and wider regions where concentration is below detection (80, 105, 164), as discussed in Section 4 and demonstrated by experimental data in **Figure 3**.

As for the resulting behaviors, intermittency and sporadicity of odor detections manifestly hamper navigation and highlight the importance of long-distance features of behavior, such as ranges of attraction, control of casting behavior and its modulation by past odor encounters, that remain largely unknown. Future progress would ideally bring techniques to interrogate the transport of small molecules in their native environments (with wind, obstacles, etc.), but methods will no doubt be easier to develop in a lab setting. Such measurements would stimulate further theoretical analysis of odor transport, and also inform the design of odor stimuli to be delivered to animals to simulate realistic situations.

above. Detecting a particular smell amid other background odors is a key task in olfaction that has parallels to other source separation problems. Algorithms based on temporal fluctuation of components (72) are compatible with turbulent transport, and there is some behavioral evidence for such separation in insects (165, 168). Whether and how mammals such as mice use this strategy is beginning to be explored (87). Source separation in the absence of time-varying cues requires other strategies, possibly including simple linear decoding under certain conditions (28, 169).

From a theoretical standpoint, learning methods offer a normative perspective on the sensory information that is most useful and the strategies that animals use to navigate effectively. The ability to control the constraints faced by a learning agent should enable a quantification of the relative importance of different computational, physiological, and physical factors on the search. Importantly, such methods offer a test bed for generating new algorithmic hypotheses and experimental predictions. Even here, challenges remain. In the model-free setting, neural network-based approaches have reached astounding success in well-controlled simulated environments (170–172). Yet, these approaches are data hungry and rely on the ability to rapidly generate millions of training examples. For olfactory navigation, training examples are limited by simulations of high Reynolds

number odor plumes, which are computationally expensive at the spatial and temporal scales relevant for olfactory searches.

A key obstacle faced by both computational and experimental paradigms is the coupling between perception and action, which underpins animal behavior and decision-making. This coupling introduces a curse-of-history situation, in which the actions of an agent depend in principle on the full history of how the agent has moved and what it has perceived. New theoretical frameworks and methodologies are required to effectively analyze and infer algorithmic aspects from behavioral data. Olfactory navigation provides a model computational task that is not only of fundamental biological importance but also encompasses the basic challenges that accompany the quantitative analysis of animal behavior.

DISCLOSURE STATEMENT

The authors are not aware of any affiliations, memberships, funding, or financial holdings that might be perceived as affecting the objectivity of this review.

ACKNOWLEDGMENTS

This research was supported in part by the National Science Foundation (NSF) under grant number NSF PHY-1748958, National Institutes of Health grant number R25GM067110, and the Gordon and Betty Moore Foundation grant number 2919.02. G.R. was partially supported by the NSF–Simons Center for Mathematical & Statistical Analysis of Biology at Harvard (award number #1764269) and the Harvard Quantitative Biology Initiative. We thank Souvik Mandal for help illustrating **Figure 1**, and Kenny Blum for his valuable comments on the manuscript.

LITERATURE CITED

1. Schneider D. 1964. *Annu. Rev. Entomol.* 9:103–22
2. Rajan R, Clement JP, Bhalla US. 2006. *Science* 311:666–70
3. Khan AG, Sarangi M, Bhalla US. 2012. *Nat. Commun.* 3:1–10
4. Bhattacharyya U, Bhalla US. 2015. *eNeuro* 2:ENEURO.0102-15.2015
5. Gire DH, Kapoor V, Arrighi-Allisan A, Seminara A, Murthy VN. 2016. *Curr. Biol.* 26:1261–73
6. Esquivelzeta Rabell J, Mutlu K, Noutel J, Martin del Olmo P, Haesler S. 2017. *Curr. Biol.* 27:1542–48
7. Wachowiak M. 2011. *Neuron* 71:962–73
8. Zhao K, Dalton P, Yang GC, Scherer PW. 2006. *Chem. Sens.* 31:107–18
9. Doorly D, Taylor D, Schroter R. 2008. *Respir. Physiol. Neurobiol.* 163:100–10
10. Craven BA, Paterson EG, Settles GS. 2010. *J. R. Soc. Interface* 7:933–43
11. Mozell MM. 1964. *Nature* 203:1181–82
12. Schoenfeld TA, Cleland TA. 2005. *Trends Neurosci.* 28:620–27
13. Scott JW, Sherrill L, Jiang J, Zhao K. 2014. *J. Neurosci.* 34:2025–36
14. Suzuki H. 1975. *J. Insect Physiol.* 21:831–47
15. Draft RW, McGill MR, Kapoor V, Murthy VN. 2018. *J. Exp. Biol.* 221:jeb185124
16. Harkema JR, Carey SA, Wagner JG. 2006. *Toxicol. Pathol.* 34:252–69
17. Pelosi P. 1994. *Crit. Rev. Biochem. Mol. Biol.* 29:199–228
18. Leal WS. 2013. *Annu. Rev. Entomol.* 58:373–91
19. Larter N, Sun J, Carlson J. 2016. *eLife* 5:e20242091103
20. Buck L, Axel R. 1991. *Cell* 65:175–87
21. Vosshall LB, Amrein H, Morozov PS, Rzhetsky A, Axel R. 1999. *Cell* 96:725–36
22. Su CY, Menuz K, Carlson J. 2009. *Cell* 139:45–59
23. Kurian SM, Naressi RG, Manoel D, Barwich A-S, Malnic B, Saraiva LR. 2021. *Cell Tissue Res.* 383:445–56
24. Pifferi S, Menini A, Kurahashi T. 2010. In *The Neurobiology of Olfaction*, ed. A Menini, pp. 203–24. Boca Raton, FL: CRC/Taylor & Francis

25. Glezer I, Malnic B. 2019. *Handb. Clin. Neurol.* 164:67–78
26. Fleischer J, Pregitzer P, Breer H, Krieger J. 2018. *Cell. Mol. Life Sci.* 75:485–508
27. Reisert J, Zhao H. 2011. *J. Gen. Physiol.* 138:303–10
28. Reddy G, Zak JD, Vergassola M, Murthy VN. 2018. *eLife* 7:e34958
29. Zak JD, Reddy G, Vergassola M, Murthy VN. 2020. *Nat. Commun.* 11:1–12
30. Inagaki S, Iwata R, Iwamoto M, Imai T. 2020. *Cell Rep.* 31:107814
31. Xu L, Li W, Voleti V, Zou DJ, Hillman EM, Firestein S. 2020. *Science* 368:eaaz5390
32. Pfister P, Smith BC, Evans BJ, Brann JH, Trimmer C, et al. 2020. *Curr. Biol.* 30:2574–87
33. Singh V, Murphy NR, Balasubramanian V, Mainland JD. 2019. *PNAS* 116:9598–603
34. Cao LH, Jing BY, Yang D, Zeng X, Shen Y, et al. 2016. *PNAS* 113:E902–11
35. Nagel KI, Wilson RI. 2011. *Nat. Neurosci.* 14:208–16
36. Gorur-Shandilya S, Demir M, Long J, Clark DA, Emonet T. 2017. *eLife* 6:e27670
37. Malnic B, Hirono J, Sato T, Buck LB. 1999. *Cell* 96:713–23
38. Wilson CD, Serrano GO, Koulakov AA, Rinberg D. 2017. *Nat. Commun.* 8:1–10
39. Holy TE. 2018. *Annu. Rev. Neurosci.* 41:501–25
40. Mafra-Neto A, Cardé RT. 1994. *Nature* 369:142–44
41. Lemon W, Getz W. 1997. *J. Exp. Biol.* 200:1809–19
42. Szyszka P, Gerkin RC, Galizia CG, Smith BH. 2014. *PNAS* 111:16925–30
43. Riffell JA, Shlizerman E, Sanders E, Abrell L, Medina B, et al. 2014. *Science* 344:1515–18
44. Geffen MN, Broome BM, Laurent G, Meister M. 2009. *Neuron* 61:570–86
45. Martelli C, Carlson JR, Emonet T. 2013. *J. Neurosci.* 33:6285–97
46. Mombaerts P, Wang F, Dulac C, Chao SK, Nemes A, et al. 1996. *Cell* 87:675–86
47. Wilson RI. 2013. *Annu. Rev. Neurosci.* 36:217–41
48. Zhang X, Firestein S. 2002. *Nat. Neurosci.* 5:124–33
49. Brann DH, Datta SR. 2020. *Annu. Rev. Neurosci.* 43:277–95
50. Gollisch T, Meister M. 2010. *Neuron* 65:150–64
51. Baden T, Berens P, Franke K, Rosón MR, Bethge M, Euler T. 2016. *Nature* 529:345–50
52. Modi MN, Shuai Y, Turner GC. 2020. *Annu. Rev. Neurosci.* 43:465–84
53. Chakraborty SD, Sachse S. 2021. *Cell Tissue Res.* 383:113–23
54. Igarashi KM, Ieki N, An M, Yamaguchi Y, Nagayama S, et al. 2012. *J. Neurosci.* 32:7970–85
55. Marin AC, Schaefer AT, Ackels T. 2021. *Cell Tissue Res.* 383:473–83
56. Yang HH, Clandinin TR. 2018. *Annu. Rev. Vis. Sci.* 4:143–63
57. Baker KL, Dickinson M, Findley TM, Gire DH, Louis M, et al. 2018. *J. Neurosci.* 38:9383–89
58. Riman N, Victor JD, Boie SD, Ermentrout B. 2021. *SIAM Rev.* 63:100–20
59. Catania KC. 2013. *Nat. Commun.* 4:1–8
60. Findley TM, Wyrick DG, Cramer JL, Brown MA, Holcomb B, et al. 2021. *eLife* 10:e58523
61. Gumaste A, Coronas-Samano G, Hengenius J, Axman R, Connor E, et al. 2020. *eNeuro* 7:ENEURO.0212-19.2019
62. Jackson BJ, Fatima GL, Oh S, Gire DH. 2020. *eNeuro* 7:ENEURO.0536-19.2020
63. Liu A, Papale AE, Hengenius J, Patel K, Ermentrout B, Urban NN. 2020. *Front. Neurosci.* 14:218
64. Park IJ, Hein AM, Bobkov YV, Reidenbach MA, Ache BW, Principe JC. 2016. *PLOS Comput. Biol.* 12:e1004682
65. Rabell JE, Mutlu K, Noutel J, Del Olmo PM, Haesler S. 2017. *Curr. Biol.* 27:1542–48
66. Gaudry Q, Hong EJ, Kain J, de Bivort BL, Wilson RI. 2013. *Nature* 493:424–28
67. Dalal T, Gupta N, Haddad R. 2020. *Commun. Biol.* 3:1–12
68. Rokni D, Hemmelder V, Kapoor V, Murthy VN. 2014. *Nat. Neurosci.* 17:1225–32
69. Haykin S, Chen Z. 2005. *Neural Comput.* 17:1875–902
70. Wilson DA. 1998. *J. Neurophysiol.* 79:1425–40
71. Shen Y, Dasgupta S, Navlakha S. 2020. *PNAS* 117:12402–10
72. Hopfield J. 1991. *PNAS* 88:6462–66
73. Lawless HT. 1997. In *Tasting and Smelling*, ed. GK Beauchamp, L Baroshuk, pp. 125–74. San Diego, CA: Academic

74. Thomas-Danguin T, Sinding C, Romagny S, El Mountassir F, Atanasova B, et al. 2014. *Front. Psychol.* 5:504
75. Lin DY, Shea SD, Katz LC. 2006. *Neuron* 50:937–49
76. Soucy ER, Albeanu DF, Fantana AL, Murthy VN, Meister M. 2009. *Nat. Neurosci.* 12:210–20
77. Vincis R, Gschwend O, Bhaukaurally K, Beroud J, Carleton A. 2012. *Nat. Neurosci.* 15:537–39
78. Oka Y, Omura M, Kataoka H, Touhara K. 2004. *EMBO J.* 23:120–26
79. Wilson DA, Stevenson RJ, Stevenson RJ, Stevenson RJ. 2006. *Learning to Smell: Olfactory Perception from Neurobiology to Behavior*. Baltimore, MD: Johns Hopkins Univ. Press
80. Celani A, Villermaux E, Vergassola M. 2014. *Phys. Rev. X* 4:041015
81. Yee E, Kosteniuk P, Chandler G, Biltoft C, Bowers J. 1993. *Boundary-Layer Meteorol.* 65:69–109
82. Acheson DJ. 1991. *J. Acoust. Soc. Am.* 89:3020
83. Aref H. 1984. *J. Fluid Mech.* 143:1–21
84. Villermaux E. 2019. *Annu. Rev. Fluid Mech.* 51:245–73
85. Taylor GI. 1922. *Proc. Lond. Math. Soc.* 2:196–212
86. Vallero DA. 2014. *Fundamentals of Air Pollution*. San Diego, CA: Academic
87. Erskine A, Ackels T, Dasgupta D, Fukunaga I, Schaefer AT. 2021. *Nature* 593:558–63
88. Sutton O. 1953. *Micrometeorology*. New York: McGraw-Hill Book Co.
89. Elkinton J, Cardé R, Mason C. 1984. *J. Chem. Ecol.* 10:1081–108
90. Murlis J, Willis MA, Cardé RT. 2000. *Physiol. Entomol.* 25:211–22
91. Kree M, Duplat J, Villermaux E. 2013. *Phys. Fluids* 25:091103. **https://doi.org/10.1063/1.4820015**
92. Frisch U. 1995. *Turbulence: The Legacy of A. N. Kolmogorov*. Cambridge, UK: Cambridge Univ. Press
93. Metzler R, Klafter J. 2000. *Phys. Rep.* 339:1–77
94. Villermaux E, Innocenti C. 1999. *J. Fluid Mech.* 393:123–47
95. McMeniman C, Corfas R, Matthews B, Ritchie S, Vosshall L. 2014. *Cell* 156:1060–71
96. van Breugel F, Riffell J, Fairhall A, Dickinson M. 2015. *Curr. Biol.* 25:2123–29
97. Cardé RT. 2015. *Curr. Biol.* 25:R793–95
98. Schreck C, Gouck H, Posey K. 1972. *Mosquito News* 32:496–501
99. Murlis J, Elkinton JS, Carde RT. 1992. *Annu. Rev. Entomol.* 37:505–32
100. Shraiman BI, Siggia ED. 2000. *Nature* 405:639–46
101. Falkovich G, Gawedzki K, Vergassola M. 2001. *Rev. Mod. Phys.* 73:912–75
102. Toschi F, Bodenschatz E. 2009. *Annu. Rev. Fluid Mech.* 41:375–404
103. Maxey MR. 1987. *J. Fluid Mech.* 174:441–65
104. Balkovsky E, Falkovich G, Fouxon A. 2001. *Phys. Rev. Lett.* 86:2790–93
105. Yee E, Chan R, Kosteniuk P, Chandler G, Biltoft C, Bowers J. 1995. *Boundary-Layer Meteorol.* 73:53–90
106. Webb B, Consilvio T. 2001. *Biorobotics*. Cambridge, MA: MIT Press
107. Berg HC. 2008. *E. coli in Motion*. New York: Springer
108. Dusenbery DB. 1997. *PNAS* 94:10949–54
109. Loomis W. 1975. *Dictyostelium Discoideum: A Developmental System*. New York: Academic
110. Levine H, Rappel W-J. 2013. *Phys. Today* 66:24
111. Pierce-Shimomura JT, Morse TM, Lockery SR. 1999. *J. Neurosci.* 19:9557–69
112. Louis M, Huber T, Benton R, Sakmar TP, Vosshall LB. 2008. *Nat. Neurosci.* 11:187–99
113. Iino Y, Yoshida K. 2009. *J. Neurosci.* 29:5370–80
114. Gomez-Marin A, Duistermars B, Frye MA, Louis M. 2010. *Front. Cell. Neurosci.* 4:6
115. Gepner R, Skanata MM, Bernat NM, Kaplow M, Gershow M. 2015. *eLife* 4:e06229
116. Hernandez-Nunez L, Belina J, Klein M, Si G, Claus L, et al. 2015. *eLife* 4:e06225
117. Schulze A, Gomez-Marin A, Rajendran VG, Lott G, Musy M, et al. 2015. *eLife* 4:e06694
118. Wu Y, Chen K, Ye Y, Zhang T, Zhou W. 2020. *PNAS* 117:16065–71
119. Stockham RA, Slavin DL, Kift W. 2004. *Forens. Sci. Commun.* 6:1–12
120. Thesen A, Steen JB, Doving K. 1993. *J. Exp. Biol.* 180:247–51
121. Hepper PG, Wells DL. 2005. *Chem. Sens.* 30:291–98
122. Jinn J, Connor EG, Jacobs LF. 2020. *Chem. Sens.* 45:625–34
123. Reddy G, Shraiman BI, Vergassola M. 2022. 119(1):e2107431118

124. Vickers NJ. 2000. *Biol. Bull.* 198:203–12
125. Vickers NJ. 2006. *Chem. Sens.* 31:155–66
126. Cardé RT, Willis MA. 2008. *J. Chem. Ecol.* 34:854–66
127. David C, Kennedy J, Ludlow A. 1983. *Nature* 303:804–6
128. Allison JD, Cardé RT, eds. 2016. *Pheromone Communication in Moths: Evolution, Behavior, and Application*. Oakland, CA: Univ. Calif. Press
129. Cardé RT. 2016. In *Pheromone Communication in Moths*, ed. JD Allison, RT Cardé, pp. 173–89. Oakland, CA: Univ. Calif. Press
130. Kennedy JS, Marsh D. 1974. *Science* 184:999–1001
131. Vickers N, Baker TC. 1996. *J. Comp. Physiol. A* 178:831–47
132. Budick SA, Dickinson MH. 2006. *J. Exp. Biol.* 209:3001–17
133. van Breugel F, Dickinson MH. 2014. *Curr. Biol.* 24:274–86
134. Willis M, Avondet J. 2005. *J. Exp. Biol.* 208:721–35
135. Lockey JK, Willis MA. 2015. *J. Exp. Biol.* 218:2156–65
136. Álvarez-Salvado E, Licata AM, Connor EG, McHugh MK, King BM, et al. 2018. *eLife* 7:e37815
137. Demir M, Kadakia N, Anderson HD, Clark DA, Emonet T. 2020. *eLife* 9:e57524
138. Duistermars BJ, Frye MA. 2010. *Commun. Integr. Biol.* 3:60–63
139. Saxena N, Natesan D, Sane SP. 2018. *J. Exp. Biol.* 221:jeb172023
140. Vergassola M, Villermaux E, Shraiman BI. 2007. *Nature* 445:406–9
141. Moraud E, Martinez D. 2010. *Front. Neurorobot.* 4:1
142. Masson JB. 2013. *PNAS* 110:11261–66
143. Masson JB, Bailly-Bechet M, Vergassola M. 2009. *J. Phys. A: Math. Theor.* 42:434009
144. Karpas E, Shklarsh A, Schneidman E. 2017. *PNAS* 114:5589–94
145. Mejia-Monasterio C, Oshanin G, Schehr G. 2011. *J. Stat. Mech.* 2011:P06022
146. Bell A, Sejnowski T. 1995. *Neural Comput.* 7:1129–59
147. Tkacik G, Walczak A. 2011. *J. Phys.: Condens. Matter* 23:153102
148. Renninger LW, Verghese P, Coughlan J. 2007. *J. Vis.* 7:6
149. Najemnik J, Geisler W. 2008. *J. Vis.* 8:1–14
150. Barbieri C, Cocco S, Monasson R. 2011. *Europhys. Lett.* 94:20005
151. Reddy G, Celani A, Vergassola M. 2016. *J. Stat. Phys.* 163:1454–76
152. Pang R, van Breugel F, Dickinson M, Riffell J, Fairhall A. 2018. *PLOS Comput. Biol.* 14:e1005969
153. Hernandez-Reyes C, Fukushima S, Shigaki S, Kurabayashi D, Sakurai T, et al. 2021. *Front. Comput. Neurosci.* 15:629380
154. Calhoun A, Chalasani S, Sharpee T. 2014. *eLife* 3:e04220
155. Kaelbling L, Littman M, Cassandra A. 1998. *Artif. Intel.* 101:99134
156. Sutton R, Barto A. 2018. *Reinforcement Learning: An Introduction*. Cambridge, MA: MIT Press. 2nd ed.
157. Bellman R. 2003. *Dynamic Programming*. Minneola, NY: Dover
158. Shani G, Pineau J, Kaplow R. 2013. *Auton. Agents Multi-Agent Syst.* 27:1–51
159. Boie SD, Connor EG, McHugh M, Nagel KI, Ermentrout GB, et al. 2018. *PLOS Comput. Biol.* 14:e1006275
160. Victor JD, Boie SD, Connor EG, Crimaldi JP, Ermentrout GB, Nagel KI. 2019. *J. Neurosci.* 39:3713–27
161. Rapp H, Nawrot MP. 2020. *PNAS* 117:28412–21
162. Crimaldi J, Koseff J. 2001. *Exp. Fluids* 31:90–102
163. Connor EG, McHugh MK, Crimaldi JP. 2018. *Exp. Fluids* 59:1–11
164. Mylne KR, Mason P. 1991. *Q. J. R. Meteorol. Soc.* 117:177–206
165. Fadamiro H, Cossé A, Baker TC. 1999. *J. Comp. Physiol. A* 185:131–41
166. Webb B, Wystrach A. 2016. *Curr. Opin. Insect Sci.* 15:27–39
167. Lever C, Burton S, O'Keefe J. 2006. *Rev. Neurosci.* 17:111–33
168. Szyszka P, Stierle JS. 2014. *Prog. Brain Res.* 208:63–85
169. Mathis A, Rokni D, Kapoor V, Bethge M, Murthy V. 2016. *Neuron* 91:1110–23
170. Levine S, Finn C, Darrell T, Abbeel P. 2016. *J. Mach. Learn. Res.* 17:1334–73
171. Mnih V, Kavukcuoglu K, Silver D, Rusu AA, Veness J, et al. 2015. *Nature* 518:529–33
172. Silver D, Schrittwieser J, Simonyan K, Antonoglou I, Huang A, et al. 2017. *Nature* 550:354–59

Annual Review of Condensed Matter Physics

Volume 13, 2022

Contents

Reflections on 65 Years of Helium Research
John D. Reppy 1

My Life and Science
Valery L. Pokrovsky 15

Russell Donnelly and His Leaks
J.J. Niemela and K.R. Sreenivasan 33

Director Deformations, Geometric Frustration, and Modulated Phases in Liquid Crystals
Jonathan V. Selinger 49

Thin Film Skyrmionics
Takaaki Dohi, Robert M. Reeve, and Mathias Kläui 73

The Physics of Dense Suspensions
Christopher Ness, Ryohei Seto, and Romain Mari 97

Topological Magnets: Functions Based on Berry Phase and Multipoles
Satoru Nakatsuji and Ryotaro Arita 119

Active Turbulence
Ricard Alert, Jaume Casademunt, and Jean-François Joanny 143

Topological Magnons: A Review
Paul A. McClarty 171

Olfactory Sensing and Navigation in Turbulent Environments
Gautam Reddy, Venkatesh N. Murthy, and Massimo Vergassola 191

Irreversibility and Biased Ensembles in Active Matter: Insights from Stochastic Thermodynamics
Étienne Fodor, Robert L. Jack, and Michael E. Cates 215

The Hubbard Model
Daniel P. Arovas, Erez Berg, Steven A. Kivelson, and Srinivas Raghu 239

The Hubbard Model: A Computational Perspective
Mingpu Qin, Thomas Schäfer, Sabine Andergassen, Philippe Corboz, and Emanuel Gull 275

Understanding Hydrophobic Effects: Insights from Water Density Fluctuations
Nicholas B. Rego and Amish J. Patel 303

Modeling of Ferroelectric Oxide Perovskites: From First to Second Principles
Philippe Ghosez and Javier Junquera 325

How Cross-Link Numbers Shape the Large-Scale Physics of Cytoskeletal Materials
Sebastian Fürthauer and Michael J. Shelley 365

Studying Quantum Materials with Scanning SQUID Microscopy
Eylon Persky, Ilya Sochnikov, and Beena Kalisky 385

Coherently Coupled Mixtures of Ultracold Atomic Gases
Alessio Recati and Sandro Stringari 407

Errata

An online log of corrections to *Annual Review of Condensed Matter Physics* articles may be found at http://www.annualreviews.org/errata/conmatphys